



## Temperature distribution in membrane-type micro-hot-plates with circular geometry

Usman Khan<sup>a</sup>, Christian Falconi<sup>a,b,\*</sup>

<sup>a</sup> Department of Electronic Engineering, University of Tor Vergata, Via del Politecnico 1, 00133 Rome, Italy

<sup>b</sup> CNR IDASC, Via Fosso del Cavaliere 100, 00133 Rome, Italy

### ARTICLE INFO

#### Article history:

Received 31 May 2012

Received in revised form

10 September 2012

Accepted 7 November 2012

Available online xxx

#### Keywords:

Micro-hot-plates

Temperature distribution

Gas sensors

Infrared emitters

Micro-reactors

### ABSTRACT

The absence of an accurate analytical model for the temperature distribution in micro-hot-plates does not allow the systematic design of micro-heaters with high temperature uniformity in the hot region, a key issue for the fabrication of accurate gas sensors, infrared emitters with high spectral purity, and micro-reactors with uniform deposition on sufficiently large areas. Here, by considering a circular heater geometry and typical (i.e. very small) thicknesses, we reduce the three-dimensional temperature distribution to one dimension only and, by solving a form of Bessel differential equation, we express the temperature distribution in terms of modified Bessel functions. The resulting relations accurately approximate the radiation heat transfer within the heater, which is a decisive advantage as the temperature within the heater is generally very high. Finally, we demonstrate that our model has almost the same accuracy as finite element method (FEM) simulations and is therefore suitable for designing micro-hot-plates with unprecedented temperature homogeneity as well as for accurately predicting the temperature profile in generic micro-hot-plates.

© 2012 Elsevier B.V. All rights reserved.

### 1. Introduction

Micro-hot-plates are micro-machined devices comprising resistive heaters; the heater is integrated within a membrane which is thermally isolated from the silicon substrate by etching [1]. As a key advantage, due to increased thermal resistance between the heater and substrate, micro-hot-plates allow one to obtain high temperature with low power consumption [2]; moreover, since the micro-hot-plate can be heated without significantly increasing the substrate temperature, other elements on the same chip (electronic interface [3], other sensors/actuators and possibly, in future, integrated energy harvesters [4–6]) can operate at much lower temperatures than the micro-hot-plate [7]. Additionally, micro-hot-plates are fast to heat and cool quickly due to their low thermal mass and may also be cheap for sufficiently large volumes [2,8]. One of the major applications of micro-hot-plates is to heat sensitive materials of chemical sensors to an optimal working temperature (e.g. in metal oxide gas sensors), with application in food analysis, medicine, and more [9,10]; however, both the selectivity and sensitivity of the sensors strongly depend on temperature within the sensing area [1,11,12] so that temperature uniformity is crucial. Furthermore, micro-hot-plates can efficiently emit infrared light

at temperatures in excess of 600–700 °C, with application in optical gas sensing systems for air quality monitoring (CO<sub>2</sub>), gas leak detection (natural gas, cooling agents, N<sub>2</sub>O), fire detection (CO<sub>2</sub>, CO) and water detection in brake and hydraulic fluids [8,13]. However, even for infrared emission, the temperature uniformity of the micro-hot-plate is crucial [14] because the emission strongly depends upon temperature. As another very promising application, micro-hot-plates can be used for growing thin films or nanostructures, e.g. by chemical vapor deposition, in micro-reactors, with possibly decisive advantages such as low cost, reduced waste of chemicals, much faster start and stop of the growth and simultaneous testing of many different experimental conditions (i.e. by using arrays of devices in a single chip) [7,15]. However, even in this case, the existence of temperature gradients unavoidably results in non-homogeneities of the thin film or nanostructures [15,16] which may be undesirable in some applications (e.g. growth of an array of nominally identical nanowires [17]).

Micro-hot-plates with simple meander shape heaters typically have a central hot spot [12] because, though the power per unit area within the heater is almost constant, there is a significant asymmetry between the central (surrounded only by other hot regions) and the peripheral parts (surrounded by both hot and cold regions) of the heater. Therefore, different strategies have been reported in literature for homogenizing the temperature distribution within the heater. A first straightforward and effective method is to include a heat spreading plate [2,7,12] which, however, increases the cost and complexity of fabrication. As another (and, eventually,

\* Corresponding author at: Department of Electronic Engineering, University of Tor Vergata, Via del Politecnico 1, 00133 Rome, Italy.

E-mail address: [falconi@eln.uniroma2.it](mailto:falconi@eln.uniroma2.it) (C. Falconi).

complementary) approach, the heater geometry can be designed so that the power per unit area within the heater is significantly non-constant (e.g. spiral heater) and can somehow compensate for the asymmetry between the central and the peripheral parts [18–22]. Additionally, it has been proposed to use two distinct heaters for separately compensating the thermal losses inside and outside heater [17,23,24]. Finally, it has also been demonstrated that two distinct temperature sensors and control loops can be used for independently controlling two temperatures in the hot-plate [23].

In the absence of a sufficiently accurate analytical model for the temperature distribution there are no systematic design methodologies for the design of micro-hot-plates with high temperature uniformity. The goal of this paper is to determine an analytical model for the temperature distribution in membrane-type micro-hot-plates which has almost the same accuracy as FEM simulations and is therefore suitable for systematic design of micro-hot-plates with substantially improved temperature uniformity as well as for allowing to easily predict the temperature profile in a micro-hot-plate once the temperature is measured (or controlled) in relevant points.

In literature, several analytical models have been proposed for predicting the temperature distribution in membrane-type micro-hot-plates [25–31]. Kozlov determined the temperature distribution in thermal micro-sensors (radiation sensors, thermal converters, metal oxide gas sensors and pellistor-type catalytic gas sensors) using the Fourier method [25,26]. However, in order to simplify the radiation heat loss as a linear function of the sensor temperature, Kozlov assumed that the temperature difference between the sensor and the environment is small; this however is not accurate for micro-hot-plates, whose temperatures are generally much higher than the environment temperature. Moreover, Kozlov did not consider the heater geometry in the heat-generating regions, which is very important, as we shall see. Similarly Völklein et al., in their model for temperature distribution in thermoelectric micro-sensors (radiation, power, flow or vacuum sensors), simplified radiation heat loss using the same assumption of small temperature difference between the environment and the sensor [28] which is not accurate for micro-hot-plates. Secondly, Völklein et al. considered heat spreading plates and, therefore, assumed a constant temperature inside the heater and determined the temperature distribution only outside the heater, which is obviously not suitable for the design of micro-hot-plates with high temperature uniformity within the heater. Similarly, Giberti et al. also assumed a constant temperature inside the heater region [29]; furthermore, despite their rectangular heater geometry, they assumed circular structural symmetry; additionally, they also ignored radiation heat losses. Similarly, Li et al. developed analytical relations for temperature distribution in micro-hot-plate using Bessel functions [30]; however they also assumed circular structural symmetry even though they adopted a rectangular micro-hot-plate structure. Additionally, Li et al. utilized a single ring heater design which is not general; moreover, they also simplified radiation loss by assuming a small temperature difference between micro-hot-plate and environment which is not correct for the typically high temperatures of micro-hot-plates. Correspondingly, Csendes et al. have determined the temperature distribution in thermally isolated structures using Fourier method [27]; nevertheless they ignored the heat lost due to radiation and convection which in fact are significant and can be decisive in micro-hot-plate design. Moreover, Jain et al. [31] have developed a model for prediction of temperature distribution in membrane-type micro-hot-plate with a line heat source; however, they assumed that the convection and radiation heat transfer are negligible, whereas, in the common micro-hot-plates, especially for gas sensing and micro-reactors, radiation and convection cannot be ignored. Moreover, the micro-hot-plate structure utilized by Jain

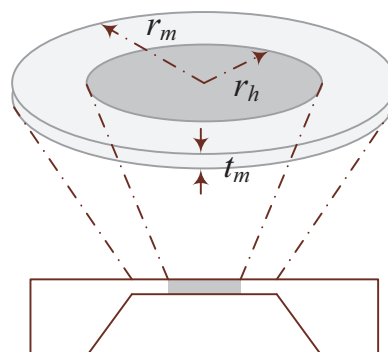


Fig. 1. Simplified representation of a micro-hot-plate (not in scale).

et al. work is unconventional as it utilizes a line heat source, which is unlike the common micro-hot-plate structures, for gas sensing, micro-reactors and infra-red emitters, which have a heater region (where an even temperature is desired) and an external region. As another important issue, none of the aforementioned models has been validated by comparison with either FEM or measured results.

Here, we consider membrane-type micro-hot-plates with circular symmetry and typical (i.e. very small) values of the thickness; with these assumptions it is possible to find a general analytical expression for the temperature distribution. Our relations are only apparently similar to other cylindrical structures like annular fins [32] however we also consider radiation heat loss within the hot region, which is crucial because of the typically high temperatures of micro-hot-plates. Afterwards, as an illustrative example, we consider a two-heater design with two important types of boundary conditions and we show how the general relations can be applied in both cases; clearly, our relations are general and can be applied to different boundary conditions as well as to other circular multi-heater designs.

## 2. Analytical modeling of temperature distribution in micro-hot-plates

We consider the micro-hot-plate schematically shown in Fig. 1, where  $t_m$  is the thickness of the membrane,  $r_m$  is the radius of the membrane, and  $r_h$  is the radius of the hot-region (i.e. the area whose temperature profile must be as close as possible to the desired one, dark-gray color in Fig. 1). We will refer to  $T_h$  as the desired temperature for the hot-region and will consider the temperature boundary condition  $T = T_a$  ( $T_a$ , ambient temperature) for the bulk [23]. In general, there are conduction heat transfer through the membrane and both convection and radiation heat transfer at both the top and the bottom surfaces of the membrane. In typical devices the temperature is very high in the heater region and, while outside of heater region, it rapidly decays toward the much lower ambient temperature,  $T_a$  at the bulk; therefore, intuitively, since radiation heat transfer greatly increases at higher temperatures [1], as a first-order approximation we may consider radiation heat loss only in the heater region. This simplification will under-estimate the heat losses outside the heater region and, therefore, will over-estimate the thermal resistance between the heater region and the bulk or, equivalently, will over-estimate the temperature in the hot region for a given heater power. Though the error in  $T_h$  can be large (e.g. even larger than 10 °C), if we restrict to the hot region, there is only a constant over-estimate error or, equivalently, a shift of the temperature distribution (in fact, inside the heater region radiation would be fully taken into account) which does not affect the evaluation of the temperature uniformity. As a consequence, for the design of micro-hot-plates with high temperature uniformity, this approximation is unimportant (as we shall verify later, see Fig. 6

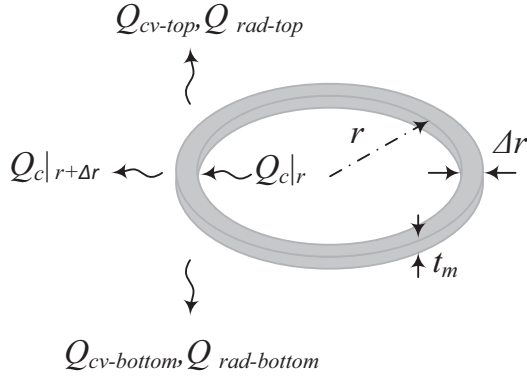


Fig. 2. Heat flows for a thin cylindrical ring.

and correspondent discussion). Similarly, obviously, this constant (in the heater region) shift is irrelevant for the prediction of the temperature profile in the heater region if the temperature is measured (or controlled) in relevant points inside the heater region.

Since, for simplicity, we consider a perfectly circular structure, as shown in Fig. 1, there is no circular temperature variation. Moreover, since the thickness  $t_m$  in a micro-hot-plate must typically be very small (in order to achieve sufficient thermal isolation between heater and substrate) the temperature variation along thickness can also be ignored. Consequently, we assume that temperature in the entire membrane only depends on the distance from the center,  $r$ ; this simplification reduces the three-dimensional temperature distribution to one dimension only.

By applying thermal energy balance to a thin cylindrical ring in micro-hot-plate (see Fig. 2) we find:

$$Q_c|_{r+\Delta r} - Q_c|_r + Q_{cv-top} + Q_{cv-bottom} + Q_{rad-top} + Q_{rad-bottom} = 0 \quad (1)$$

where  $Q_c$  is the heat flow due to conduction,  $Q_{cv-top}$  and  $Q_{cv-bottom}$  are the convection heat flows from the top and bottom surfaces,  $Q_{rad-top}$  and  $Q_{rad-bottom}$  are the radiation heat flows from the top and bottom surfaces. The conduction, convection, and radiation heat flows may be expressed as [32]:

$$Q_c = q_c(2\pi r t_m) \quad (2)$$

$$Q_{cv-top} + Q_{cv-bottom} = h_c(2\pi r \Delta r)(T - T_a) \quad (3)$$

$$Q_{rad-top} + Q_{rad-bottom} = \sigma \varepsilon(2\pi r \Delta r)(T^4 - T_a^4) \quad (4)$$

where  $\sigma$  is Stefan's Boltzmann constant,  $q_c$  is heat flux for conduction in the radial direction,  $2\pi r t_m$  is cross sectional area for conduction,  $2\pi r \Delta r$  is the surface area for convection and radiation,  $\varepsilon$  is the average surface emissivity of membrane and  $h_c$  is the average convection heat transfer coefficient (average refers to the top and bottom surfaces which, in general, may have different emissivities and convection heat transfer coefficients). The convection heat transfer coefficient  $h_c$  is rather difficult to predict (e.g. it strongly depends on micro-hot-plate geometry, packaging, environment, etc. [33]) and therefore must be determined prior to using our method. In literature, several methods have been utilized, including both FEM simulations and/or experiments [24,33,34]; for our simulations we have utilized the values reported in Ref. [35].

Since we are considering radiation loss only within the hot region, if the micro-hot-plate is properly designed for high temperature uniformity (i.e. the temperature in the heater is almost constant and equal to the average temperature in the heater area,  $T_h$ ), by taking advantage of the first-order Taylor series expansion centered at  $T = T_h$ , we can linearize,

$$[T^4 - T_a^4] \simeq 4T_h^3 \left[ T - \left( \frac{3T_h}{4} + \frac{T_a^4}{4T_h^3} \right) \right]. \quad (5)$$

The error of this approximation will be especially small if the temperature variations around the reference temperature  $T_h$  are very small which will be the case for a micro-hot-plate designed for maximum temperature uniformity.

Therefore, putting (5) into (4) we find that the radiation loss within heater area is, approximately, a linear function of  $T$ , so that,

$$Q_{rad-top} + Q_{rad-bottom} = \sigma \varepsilon(2\pi r \Delta r)(4T_h^3) \left[ T - \left( \frac{3T_h}{4} + \frac{T_a^4}{4T_h^3} \right) \right] \quad (6)$$

Now, having simplified the relation for radiation loss, we substitute the terms from (2), (3) and (6) into the expression for thermal energy balance (1),

$$q_c(2\pi r t_m)|_{r+\Delta r} - q_c(2\pi r t_m)|_r + 2h_c(2\pi r \Delta r)[T - T_a] + 2\sigma \varepsilon((2\pi r \Delta r))(4T_h^3) \left[ T - \left( \frac{3T_h}{4} + \frac{T_a^4}{4T_h^3} \right) \right] = 0. \quad (7)$$

Dividing (7) by  $2\pi \Delta r t_m$ , rearranging and taking the limit as  $\Delta r$  tends to zero, we obtain:

$$\lim_{\Delta r \rightarrow 0} \frac{q_c r|_{r+\Delta r} - q_c r|_r}{\Delta r} + \frac{2h_c r}{t_m} [T - T_a] + \frac{2\sigma \varepsilon r(4T_h^3)}{t_m} \left[ T - \left( \frac{3T_h}{4} + \frac{T_a^4}{4T_h^3} \right) \right] = 0. \quad (8)$$

Using the definition of derivative, we get:

$$\frac{d}{dr}(q_c r) + \frac{2h_c r}{t_m} [T - T_a] + \frac{2\sigma \varepsilon r(4T_h^3)}{t_m} \left[ T - \left( \frac{3T_h}{4} + \frac{T_a^4}{4T_h^3} \right) \right] = 0. \quad (9)$$

Substituting  $q_c = -k[dT(r)/dr]$  (Fourier's law for heat conduction [32] where  $k$  is the thermal conductivity of the membrane), into (9) and rearranging:

$$\frac{d}{dr} \left( r \frac{dT}{dr} \right) - \frac{2h_c r}{kt_m} [T - T_a] - \frac{2\sigma \varepsilon r(4T_h^3)}{kt_m} \left[ T - \left( \frac{3T_h}{4} + \frac{T_a^4}{4T_h^3} \right) \right] = 0. \quad (10)$$

Now, it is useful to rewrite (10) as:

$$\frac{d}{dr} \left( r \frac{dT}{dr} \right) - \frac{(2h_c + 8\sigma \varepsilon T_h^3)r}{kt_m} \left( T - \frac{(2h_c T_a + 6\sigma \varepsilon T_h^4 + 2\sigma \varepsilon T_a^4)}{(2h_c + 8\sigma \varepsilon T_h^3)} \right) = 0. \quad (11)$$

As a result, if we define,

$$T_o = \frac{2h_c T_a + 6\sigma \varepsilon T_h^4 + 2\sigma \varepsilon T_a^4}{2h_c + 8\sigma \varepsilon T_h^3}, \quad (12)$$

we find:

$$\frac{d}{dr} \left( r \frac{dT}{dr} \right) - \frac{(2h_c r + 8\sigma \varepsilon T_h^3)}{kt_m} [T - T_o] = 0. \quad (13)$$

If we now define  $\Delta T = T - T_o$  and apply the chain rule, we get:

$$\frac{d^2(\Delta T)}{dr^2} + \frac{1}{r} \frac{d(\Delta T)}{dr} - \frac{(2h_c + 8\sigma \varepsilon T_h^3)\Delta T}{kt_m} = 0. \quad (14)$$

This is a form of Bessel's differential equation of zero order and has a general solution [32],

$$\Delta T(r) = C_1 I_0(n_o r) + C_2 K_0(n_o r) \quad (15)$$

where  $n_o = \sqrt{(2h_c + 8\sigma \varepsilon T_h^3)/kt_m}$ ,  $C_1$  and  $C_2$  = constants that must be determined by applying the boundary conditions,  $I_i$  = modified Bessel function of 1st kind and  $i$ -th order, where

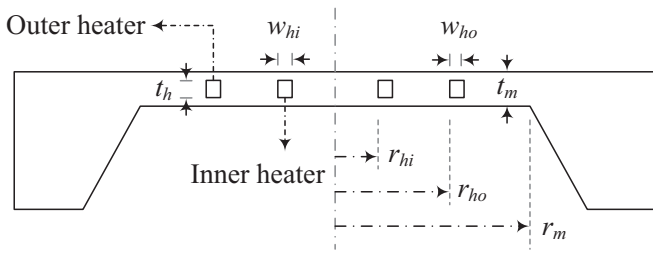


Fig. 3. Cross-sectional view of a micro-hot-plate (not in scale).

$[dl_0(n_0r)/dr] = n_0I_1(n_0r)$  [32,36], and  $K_i$  = modified Bessel function of 2nd kind and  $i$ -th order, where  $[dK_0(n_0r)/dr] = -n_0K_1(n_0r)$  [32,36].

This is a general expression for temperature distribution in a circular micro-hot-plate (see Fig. 1), where radiation heat losses outside the hot region have been ignored (the temperature outside the heater is not always very close to  $T_h$ , so the Taylor approximation (5) may not be used). As we discussed before, this corresponds to over-estimating the average temperature in the hot area,  $T_h$ , but does not affect the evaluation of the temperature uniformity. Moreover, this simplification is unimportant for the design of micro-hot-plates with high temperature uniformity (see Fig. 6 and correspondent discussion) as well as for predicting the temperature profile once the temperatures in relevant points are measured. We mention that (15) is similar to the expression found for temperature distribution in annular fins [32], but, as a decisive advantage, takes into account the radiation heat transfer inside the heater which is crucial for the typically high temperatures of micro-hot-plates.

Fig. 3 shows the cross-section of a circular micro-hot-plate using the two-heaters approach [17,23,24], i.e. there are two ring-shaped heaters. For clarity, we refer to the temperatures of the inner and outer heaters as  $T_{hi}$  and  $T_{ho}$ , respectively; for high-uniformity design, these temperatures should be close. For simplicity, we shall refer to inner and outer heaters; in practice, the inner and outer rings may be connected in series or in parallel. With such two-rings geometry, the micro-hot-plate comprises five regions: a central region inside the inner heater; the inner heater region; an intermediate region between the inner and the outer heaters; the outer heater region; an external region outside the outer heater (the heater comprises central region, inner heater region, intermediate region and outer heater region). Since, ideally, all these regions have a circular symmetry (and sufficiently small thickness, so we can neglect the temperature variations along the thickness), if we ignore radiation loss outside the heater and linearize the temperature dependence of the radiation heat flow inside the heater, the general expression (15) can be used for each region, provided the correct boundary conditions are applied. This methodology can obviously be applied to arbitrary numbers of rings.

For simplicity, though we are interested in the temperature profile inside the heater (and, therefore, cannot assume the temperature in the heater is constant), we assume that: the temperature within the inner heater is constant; the temperature within the outer heater is also constant; the temperatures of both the inner and outer heaters are known. In practice, these assumptions correspond to considering the inner and outer heaters as ideal temperature sources. In fact, first, since the heaters temperatures can be independently measured by distinct temperature sensors or even independently controlled by distinct control loops [23], we may assume that the heaters temperatures can be measured or controlled with reasonable accuracy. Furthermore, the hypothesis on constant temperatures within the heaters greatly simplifies our simulations by avoiding the introduction of electrical contacts (which would unavoidably somehow perturb the circular symmetry, a problem we do not deal within this paper) and may also be partially justified, in case the heater thickness is sufficient, by

the very high thermal conductivities of typical heaters materials (often metals). Though simplified, this scenario is sufficient for FEM validation of our model; moreover, the expression (15) is general and can also be used without this simplification (for two heaters as well as for arbitrary ring-shaped multi-heaters structures), provided the heaters are designed in such a way that circular symmetry is accurately preserved.

With the resulting three-regions simplified structure, we can easily determine the analytical expressions for the temperature, which, in practice, corresponds to applying proper boundary conditions for finding specific solutions from the general solution (15). Here, as two important illustrative examples, we consider two distinct types of boundary conditions: as a first type, case (a), we consider that the two temperatures at inner and outer heaters are arbitrarily defined (for high-uniformity design, these temperatures should be equal, but, for generality, we consider two arbitrary temperatures); as a second type, case (b), we consider the design methodology proposed in [23,24], which consists in nulling the conduction heat transfer at the inner extremity of the outer heater. Though the case (b) approach has been proposed [24] for high-temperature uniformity, here we observe that case (a) boundary conditions are better for temperature uniformity as they correspond to zero the linear dependence on the radius of the temperature profile between the inner and outer heater (i.e. the linear term is zeroed and only "higher-order" terms are left, similar to the design of bandgap voltage references [37] where zeroing the linear dependence on temperature results in a smaller voltage variation). Though case (b) may not be ideal for temperature uniformity, it may still be useful in other applications and is therefore a second significant example for the validation of our model.

Therefore, below we separately consider the three-regions and, for each region, we apply both the types of boundary conditions (BC) and determine the temperature distribution (in practice, the only difference between cases (a) and (b) is found in the intermediate region, so in the central and external region there is no need to distinguish between cases (a) and (b)).

**Central region** ( $0 \leq r \leq r_{hi}$ ) (for both the cases (a) and (b)).

BC – I: The circular symmetry gives:

$$\left. \frac{dT}{dr} \right|_{r=0} = 0$$

BC – II: The temperature at the inner heater is:

$$T(r) \Big|_{r=r_{hi}} = T_{hi}$$

Solving the general expression (15) with the previous boundary conditions, we find:

$$C_1 = \frac{T_{hi} - T_0}{I_0(n_0r_{hi})} \quad C_2 = 0. \quad (16)$$

Substituting the constants from (16) into (15) we get,

$$T(r) = \frac{(T_{hi} - T_0)}{I_0(n_0r_{hi})} I_0(n_0r) + T_0 \quad (17)$$

which is, in both cases (a) and (b), the temperature distribution in the central region.

**Intermediate region** ( $r_{hi} + w_{hi} \leq r \leq r_{ho}$ ). In both cases (a) and (b) we find:

BC – I: Temperature at the inner heater is  $T_{hi}$ .

$$T(r) \Big|_{r=r_{hi}+w_{hi}} = T_{hi}$$

BC – II: Case (a) – In case (a), we also know the temperature at the outer heater  $T_{ho}$ ,

$$T(r)|_{r=r_{ho}} = T_{ho}$$

Therefore, we may find the constants  $C_1$  and  $C_2$ ,

$$C_1 = \left[ \frac{(T_{hi} - T_o)K_0(n_o r_{ho}) - (T_{ho} - T_o)K_0(n_o(r_{hi} + w_{hi}))}{I_0(n_o(r_{hi} + w_{hi}))K_0(n_o r_{ho}) - I_0(n_o r_{ho})K_0(n_o(r_{hi} + w_{hi}))} \right]$$

$$C_2 = - \left[ \frac{(T_{hi} - T_o)I_0(n_o r_{ho}) - (T_{ho} - T_o)I_0(n_o(r_{hi} + w_{hi}))}{[I_0(n_o(r_{hi} + w_{hi}))K_0(n_o r_{ho}) - I_0(n_o r_{ho})K_0(n_o(r_{hi} + w_{hi}))]} \right]. \tag{18}$$

Substituting such values into (15) we get:

$$T(r) = \left( \frac{[(T_{hi} - T_o)K_0(n_o r_{ho}) - (T_{ho} - T_o)K_0(n_o(r_{hi} + w_{hi}))]I_0(n_o r)}{[I_0(n_o(r_{hi} + w_{hi}))K_0(n_o r_{ho}) - I_0(n_o r_{ho})K_0(n_o(r_{hi} + w_{hi}))]} - \frac{[(T_{hi} - T_o)I_0(n_o r_{ho}) - (T_{ho} - T_o)I_0(n_o(r_{hi} + w_{hi}))]K_0(n_o r)}{[I_0(n_o(r_{hi} + w_{hi}))K_0(n_o r_{ho}) - I_0(n_o r_{ho})K_0(n_o(r_{hi} + w_{hi}))]} \right) + T_o \tag{19}$$

This is, in case (a), the expression for temperature distribution in the intermediate region of the micro-hot-plate for a defined temperature  $T_{ho}$  at outer heater.

Case (b) – In case (b), at the inner extremity of the outer heater, there is no conduction heat flow toward the inner heater [23,24] that is,

$$Q_c|_{r=r_{ho}} = q_c(2\pi r t_m)|_{r=r_{ho}} = -k(2\pi r t_m) \frac{dT}{dr} \Big|_{r=r_{ho}} = 0$$

Solving (15) for two boundary conditions, the constants  $C_1$  and  $C_2$  are given by,

$$C_1 = \frac{(T_{hi} - T_o)K_1(n_o r_{ho})}{I_0(n_o(r_{hi} + w_{hi}))K_1(n_o r_{ho}) + I_1(n_o r_{ho})K_0(n_o(r_{hi} + w_{hi}))}$$

$$C_2 = \frac{(T_{hi} - T_o)I_1(n_o r_{ho})}{I_0(n_o(r_{hi} + w_{hi}))K_1(n_o r_{ho}) + I_1(n_o r_{ho})K_0(n_o(r_{hi} + w_{hi}))}. \tag{20}$$

Substituting values of the constants from (20) into (15) we get:

$$T(r) = \left( \frac{(T_{hi} - T_o)[K_1(n_o r_{ho})I_0(n_o r) + I_1(n_o r_{ho})K_0(n_o r)]}{I_0(n_o(r_{hi} + w_{hi}))K_1(n_o r_{ho}) + I_1(n_o r_{ho})K_0(n_o(r_{hi} + w_{hi}))} \right) + T_o. \tag{21}$$

This is, in case (b), the expression for temperature distribution in the intermediate region of the micro-hot-plate designed, according to Refs. [23,24] so that no conduction heat flows from the inner extremity of the outer heater toward the inner heater area. For this design, the temperature at the outer heater can be found using (21), i.e.

$$T_{ho} = T(r)|_{r=r_{ho}}. \tag{22}$$

**External region** ( $r_{ho} + w_{ho} \leq r \leq r_m$ ) (for both the cases (a) and (b)).

BC – I: The temperature at the outer heater is  $T_{ho}$ .

$$T(r)|_{r=r_{ho}+w_{ho}} = T_{ho}$$

BC – II: The membrane edge is at ambient temperature  $T_a$ , which is the temperature of the silicon substrate [23].

$$T(r)|_{r=r_m} = T_a$$

Since radiation heat loss is ignored in the external region, we may rewrite the general expression (15) without heat radiation i.e.  $\varepsilon \rightarrow 0$ , so that,

$$T(r) = C_1 I_0(n_a r) + C_2 K_0(n_a r) + T_a, \quad n_a = \sqrt{\frac{2hc}{kt_m}} \tag{23}$$

Solving (23) with the correspondent boundary conditions, the constants  $C_1$  and  $C_2$  are:

$$C_1 = \frac{(T_{ho} - T_a)K_0(n_a r_m)}{I_0(n_a(r_{ho} + w_{ho}))K_0(n_a r_m) - I_0(n_a r_m)K_0(n_a(r_{ho} + w_{ho}))}$$

$$C_2 = \frac{-(T_{ho} - T_a)I_0(n_a r_m)}{I_0(n_a(r_{ho} + w_{ho}))K_0(n_a r_m) - I_0(n_a r_m)K_0(n_a(r_{ho} + w_{ho}))}. \tag{24}$$

Replacing (24) into (23) we get,

$$T(r) = \left( \frac{(T_{ho} - T_a)[K_0(n_a r_m)I_0(n_a r) - I_0(n_a r_m)K_0(n_a r)]}{I_0(n_a(r_{ho} + w_{ho}))K_0(n_a r_m) - I_0(n_a r_m)K_0(n_a(r_{ho} + w_{ho}))} \right) + T_a. \tag{25}$$

This is, in both cases (a) and (b), the temperature distribution in the external region of the micro-hot-plate. In conclusion, the relations (17), (19)/(21) and (25), together with the assumption of constant temperatures within the heaters, constitute an approximate analytical model for the temperature distribution in a circular micro-hot-plate with two-ring-heaters. Importantly, our relations are general and apply to any multi-heater micro-hot-plate (provided the heaters are designed in such a way that the circular symmetry is accurately preserved) because a generic multi-heater micro-hot-plate has a central region inside the innermost heater (i.e. same as our central region), has an external region outside the outermost heater (i.e. same as our external region), and has some intermediate regions between the adjacent heaters (i.e. same as our intermediate region).

### 3. Comparison with FEM simulations

Since our model uses two simplifications (radiation heat transfer ignored in the external region and radiation heat transfer by its first order Taylor polynomial within the heater), in this section, we compare our model with FEM simulations carried out in COMSOL. In COMSOL, we utilized the heat transfer module and a swept mesh method with the free triangular mesh at the source faces; the triangular mesh has a maximum element size equal to 2  $\mu\text{m}$  in the heater regions, while, the mesh becomes coarser moving away from the heaters in order to reduce the computation time.

We consider an ideal micro-hot-plate with perfectly circular inner and outer heaters. For our comparison, both FEM simulations and our approximate model utilize the structure shown in Fig. 3; the membrane consists of stacked silicon dioxide and silicon nitride (with 0.35  $\mu\text{m}$  silicon dioxide at the bottom and 1.35  $\mu\text{m}$  silicon nitride); the heater is made up of platinum; the material properties are summarized in Table 1. Since the membrane is a stack of materials the analytical model determines thermal conductivity of the region  $j$  using the expression [25],

$$k_e^j = \frac{\sum_{i=1}^n a_i^j t_i^j k_i^j}{t_e^j} \quad t_e^j = \sum_{i=1}^n a_i^j t_i^j \tag{26}$$

where  $a_i^j$  is the ratio of the area of layer  $i$  in the region  $j$  to the total area of the region,  $t_i^j$  and  $k_i^j$  are the thickness and thermal conductivity, respectively, of layer  $i$  in region  $j$  and  $t_e^j$  is the effective thickness of region  $j$ . Moreover, we replaced the substrate with a temperature boundary condition  $T = T_a$  [23] with  $T_a = 20^\circ\text{C}$ . The convection heat

**Table 1**  
Material properties.

Material	Thermal conductivity [W/(mK)]	Resistivity [ $\Omega$ m]	Temperature coefficient of resistance [1/K]	Surface emissivity
Silicon dioxide	1.4	–	–	0.5 [13]
Silicon nitride	20	–	–	0.9 [39]
Platinum	71.6	$1.05 \times 10^{-7}$	$3.927 \times 10^{-3}$	–

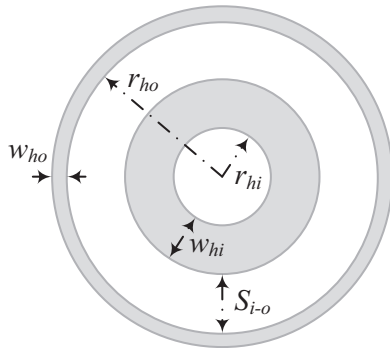


**Fig. 4.** Heater geometry (not in scale).

transfer coefficient is assumed to be equal to  $250 \text{ W}/(\text{m}^2 \text{ K})$  at the top surface and to  $150 \text{ W}/(\text{m}^2 \text{ K})$  at the bottom surface [35].

In this comparison, FEM simulations utilize the perfectly circular heaters, shown in Fig. 4; the heaters act as ideal temperature sources which is realized by applying a temperature boundary condition along their surface; all the relevant parameters are summarized in Table 2.

With reference to case (a), Fig. 5 compares our model and FEM simulations for the temperature distribution along the radius of the micro-hot-plate, with  $T_{hi} = T_{ho} = 800^\circ\text{C}$ . Due to the non-zero thickness, we consider the FEM temperatures at the same “thickness level” (i.e. distance from the top surface of the membrane) as the level of the top surface of the heaters. We have deliberately performed this comparison at very high temperatures so that radiation heat transfer is significant. In order to verify the impact of radiation heat transfer, we present FEM simulations taking into account radiation heat transfer (green-triangle curve) and FEM simulations ignoring radiation heat transfer (red-circle curve). The figure also shows the average temperature,  $T_{avg}$ , within the heater and  $\Delta T_h$  is the maximum temperature difference within the heater. FEM simulations and analytical results are practically identical. Fig. 6 shows the error of the proposed model and, for comparison, the error of FEM simulations ignoring radiation (in both cases we assume that the FEM simulations considering radiation everywhere, i.e. the most accurate possible FEM simulations, give the correct temperature distribution); obviously, the error is zero in correspondence of the heaters (ideal temperature sources assumption). Fig. 6 clearly shows that our model accurately takes into account radiation within the heater and also gives the same error as the FEM simulations ignoring radiation in the external region (in fact, our model ignores radiation in the external region). The

**Table 2**  
Micro-hot-plates parameters utilized in the comparison.

Parameters	Case (a) design [ $\mu\text{m}$ ]	Case (b) design [ $\mu\text{m}$ ]
$r_m$	750	750
$t_m$	1.7	1.7
$t_h$	0.3	0.3
$r_{hi}$	90.5	130.5
$r_{ho}$	248	248
$w_{hi}$	30.5	30.5
$w_{ho}$	4	3
$S_{i-o}$	127	87

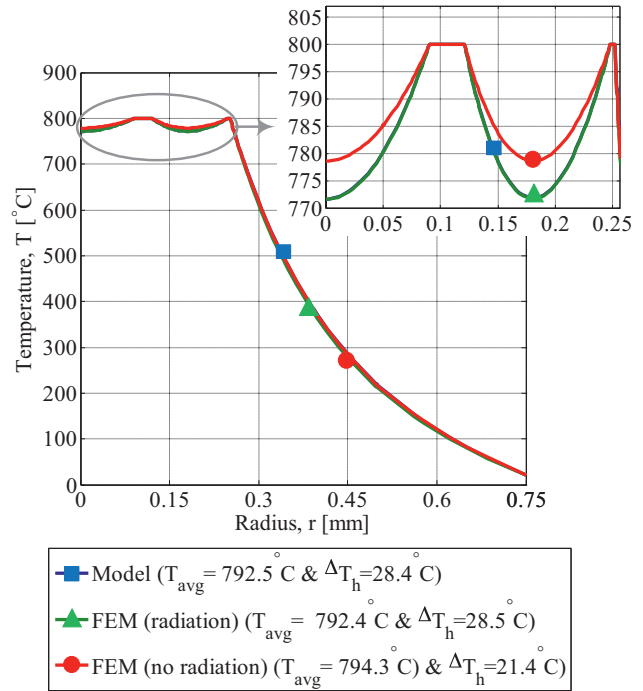


**Fig. 5.** Temperature distribution in the micro-hot-plate based on case (a) design.

relatively large error (anyway below a few  $^\circ\text{C}$ ) in the external region is insignificant if the temperatures of the heaters are accurately measured or controlled by proper feedback loops, e.g. [23,38] and is also unimportant for the evaluation of the temperature uniformity within the heater region (the values for  $\Delta T_h$  predicted by our model and by FEM simulations taking into account radiations are almost identical).

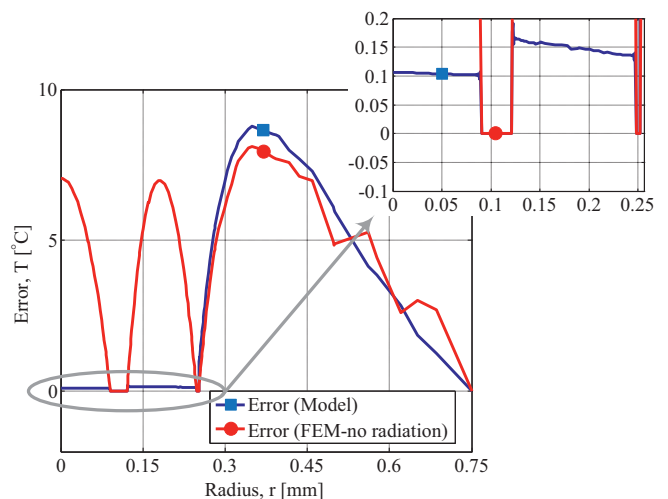


**Fig. 6.** Error between model and FEM (complete simulation, including radiation) and error between FEM (with radiation ignored) and FEM (complete simulation, including radiation) for case (a) design.

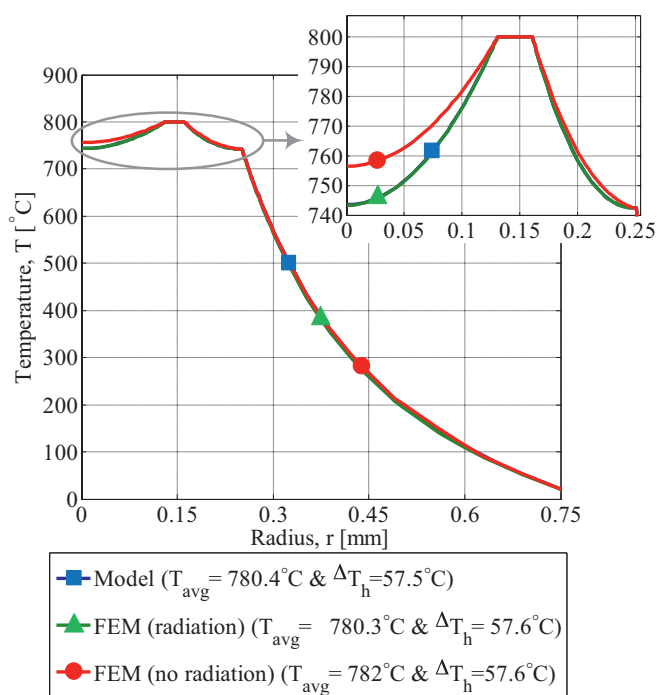


Fig. 7. Temperature distribution in the micro-hot-plate based on case (b) design.

Figs. 7 and 8 show the correspondent simulations for case (b) design with  $T_{hi} = 800^\circ\text{C}$ ,  $Q_c|_{r=r_{ho}} = 0$ .

Figs. 6 and 8 show that in both cases (a) and (b) ignoring, in FEM simulations, the radiation heat transfer within the heater region introduces large errors and thus demonstrate that our model is substantially more accurate than all previous analytical models (as discussed in Section 1, no previous analytical model accurately considered radiation heat transfer inside the heater).

The comparison of Figs. 5 and 7 also confirms that case (a) results in better temperature uniformity.

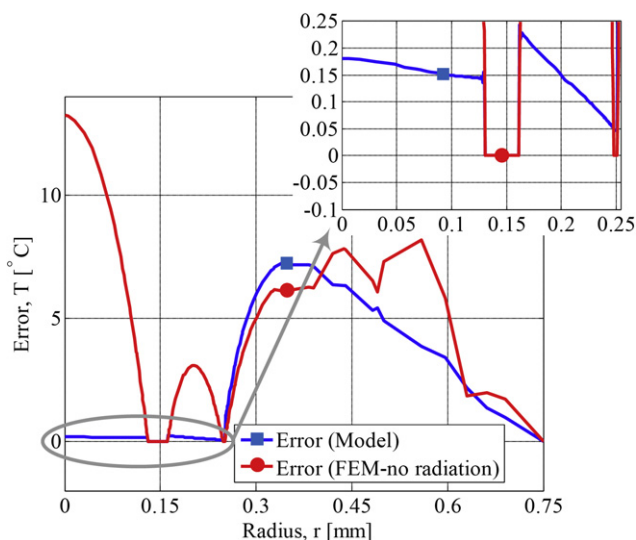


Fig. 8. Error between model and FEM (complete simulation, including radiation) and error between FEM (with radiation ignored) and FEM (complete simulation, including radiation) for case (b) design.

## 4. Conclusions

Though micro-hot-plates have been widely used for decades, there was no accurate analytical model for the temperature distribution within micro-hot-plates and, for accurate predictions, only FEM simulations are available. However, clearly, FEM simulations do not provide insight for the design, especially for the optimization of the temperature uniformity within the heater, which may be crucial for many applications, including gas sensing, infrared emitters, and micro-reactors.

Here we have developed an approximate model for the temperature distribution in membrane-type micro-hot-plates with circular heater geometry. First, by taking advantage of the typically very small thickness and of circular heater geometry, we reduced our three dimensional problem to the solution of a form of Bessel differential equation; as a result, the general solution, which is valid in each region of the micro-hot-plate, can be expressed in terms of the modified Bessel functions. Very importantly, our model accurately approximates radiation heat transfer within the heater (which is crucial for micro-hot-plates operating at very high temperature, e.g. infrared emitters). By comparison with FEM simulations we have demonstrated that, unlike all the previous analytical models for the temperature distribution in micro-hot-plates, our model is almost as accurate as FEM simulations. Moreover, the analytical relations are simple and, therefore, may provide insight for designing micro-hot-plates with unprecedented temperature uniformity or allow to easily predict the temperature profile in a generic micro-hot-plate once relevant temperatures are measured or controlled.

## Acknowledgments

This research has been supported by the Italian Institute of Technology (Project Seed – API NANE) and by the Ministero degli Affari Esteri (Direzione Generale per la Promozione e la Cooperazione Culturale). The authors acknowledge Francesco Gatta, Jyoti Prakash Kar, Andrea Orsini, and Prof. Arnaldo D'Amico for useful discussions.

## References

- [1] I. Simon, N. Bärsan, M. Bauer, U. Weimar, Micromachined metal oxide gas sensors: opportunities to improve sensor performance, *Sensors and Actuators B: Chemical* 73 (2001) 1–26.
- [2] M.Y. Afridi, J.S. Suehle, M.E. Zaghoul, D.W. Berning, A.R. Hefner, R.E. Cavicchi, S. Semancik, C.B. Montgomery, C.J. Taylor, A monolithic CMOS microhotplate-based gas sensor system, *IEEE Sensors Journal* 2 (2002) 644–655.
- [3] C. Falconi, E. Martinelli, C. Di Natale, A. D'Amico, F. Maloberti, P. Malcovati, A. Baschiroto, V. Stornelli, G. Ferri, Electronic interfaces, *Sensors and Actuators B: Chemical* 121 (2007) 295–329.
- [4] Z.L. Wang, J. Song, Piezoelectric nanogenerators based on zinc oxide nanowire arrays, *Sciences (New York, N.Y.)* 312 (2006) 242–246.
- [5] G. Romano, G. Mantini, A. Di Carlo, A. D'Amico, C. Falconi, Z.L. Wang, Piezoelectric potential in vertically aligned nanowires for high output nanogenerators, *Nanotechnology* 22 (2011) 465401.
- [6] R. Araneo, G. Lovat, P. Burghignoli, C. Falconi, Piezo-semiconductive quasi-1D nanodevices with or without anti-symmetry, *Advanced Materials* 24 (2012) 4719–4724.
- [7] R.E. Cavicchi, S. Semancik, F. DiMeo Jr., C.J. Taylor, Use of microhotplates in the controlled growth and characterization of metal oxides for chemical sensing, *Journal of Electroceramics* 9 (2002) 155–164.
- [8] J. Hildenbrand, J. Korvink, J. Wöllenstein, C. Peter, A. Kurzinger, F. Naumann, M. Elbert, F. Lamprecht, Micromachined mid-infrared emitter for fast transient temperature operation for optical gas sensing systems, *IEEE Sensors Journal* 10 (2010) 353–362.
- [9] E. Martinelli, C. Falconi, A. D'Amico, C. Di Natale, Feature extraction of chemical sensors in phase space, *Sensors and Actuators B: Chemical* 95 (2003) 132–139.
- [10] C. Falconi, C. Di Natale, E. Martinelli, A. D'Amico, E. Zampetti, J.W. Gardner, C.M. Van Vliet,  $1/f$  noise and its unusual high-frequency deactivation at high biasing currents in carbon black polymers with residual  $1/f\gamma$  ( $\gamma = 2.2$ ) noise and a preliminary estimation of the average trap energy, *Sensors and Actuators B: Chemical* 174 (2012) 577–585.
- [11] E. Martinelli, D. Polese, A. Catini, A. D'Amico, C. Di Natale, Self-adapted temperature modulation in metal-oxide semiconductor gas sensors, *Sensors and Actuators B: Chemical* 161 (2012) 534–541.

- [12] D. Briand, S. Heimgartner, M.-A. Grétilat, B. van der Schoot, N.F. de Rooij, Thermal optimization of micro-hotplates that have a silicon island, *Journal of Micromechanics and Microengineering* 12 (2002) 971–978.
- [13] O. Schulz, G. Müller, M. Lloyd, A. Ferber, Impact of environmental parameters on the emission intensity of micromachined infrared sources, *Sensors and Actuators A: Physical* 121 (2005) 172–180.
- [14] P. Barritault, M. Brun, S. Gidon, S. Nicoletti, Mid-IR source based on a free-standing microhotplate for autonomous CO<sub>2</sub> sensing in indoor applications, *Sensors and Actuators A: Physical* 172 (2011) 379–385.
- [15] B.D. Sosnowchik, L. Lin, O. Englander, Localized heating induced chemical vapor deposition for one-dimensional nanostructure synthesis, *Journal of Applied Physics* 107 (2010) 051101–051114.
- [16] K. Møhlhave, B.A. Wacaser, D.H. Petersen, J.B. Wagner, L. Samuelson, P. Bøggild, Epitaxial integration of nanowires in microsystems by local micrometer-scale vapor-phase epitaxy, *Small* 4 (2008) 1741–1746.
- [17] S.Z. Ali, S. Santra, I. Haneef, C. Schwandt, R.V. Kumar, W.I. Milne, F. Udrea, P.K. Guha, J.A. Covington, J.W. Gardner, V. Garofalo, Nanowire hydrogen gas sensor employing CMOS micro-hotplate, in: *Proceedings of IEEE Sensors Conference, IEEE, 2009*, pp. 114–117.
- [18] S. Lee, D. Dyer, J. Gardner, Design and optimisation of a high-temperature silicon micro-hotplate for nanoporous palladium pellistors, *Microelectronics Journal* 34 (2003) 115–126.
- [19] R. Aigner, M. Dietl, R. Katterloher, V. Klee, Si-planar-pellistor: designs for temperature modulated operation, *Sensors and Actuators B: Chemical* 33 (1996) 151–155.
- [20] V. Guidi, G. Carlo Cardinali, L. Dori, G. Faglia, M. Ferroni, G. Martinelli, P. Nelli, G. Sberveglieri, Thin-film gas sensor implemented on a low-power-consumption micromachined silicon structure, *Sensors and Actuators B: Chemical* 49 (1998) 88–92.
- [21] S. Astié, A.M. Gué, E. Scheid, L. Lescouzères, Optimization of an integrated SnO<sub>2</sub> gas sensor using a FEM simulator, *Sensors and Actuators A* 69 (1998) 205–211.
- [22] J. Laconte, C. Dupont, D. Flandre, J.-P. Raskin, SOI CMOS compatible low-power microheater optimization for the fabrication of smart gas sensors, *IEEE Sensors Journal* 4 (2004) 670–680.
- [23] P. Hille, H. Strack, A heated membrane for a capacitive gas sensor, *Sensors and Actuators A: Physical* 32 (1992) 321–325.
- [24] S.Z. Ali, F. Udrea, W.I. Milne, J.W. Gardner, Tungsten-based SOI microhotplates for smart gas sensors, *Journal of Microelectromechanical Systems* 17 (2008) 1408–1417.
- [25] A. Kozlov, Analytical modelling of steady-state temperature distribution in thermal microsensors using Fourier method. Part 1: theory, *Sensors and Actuators A: Physical* 101 (2002) 283–298.
- [26] A.G. Kozlov, Analytical modelling of steady-state temperature distribution in thermal microsensors using Fourier method. Part 2: practical application, *Sensors and Actuators A: Physical* 101 (2002) 299–310.
- [27] A. Csendes, V. Székely, M. Rencz, An efficient thermal simulation tool for ICs, microsystem elements and MCMs: the  $\mu$ S-THERMANAL, *Microelectronics Journal* 29 (1998) 241–255.
- [28] F. Völklein, H. Baltes, Optimization tool for the performance parameters of thermoelectric microsensors, *Sensors and Actuators A: Physical* 36 (1993) 65–71.
- [29] A. Giberti, V. Guidi, D. Vincenzi, A study of heat distribution and dissipation in a micromachined chemoresistive gas sensor, *Sensors and Actuators B: Chemical* 153 (2011) 409–414.
- [30] T. Li, L. Wu, Y. Liu, L. Wang, Y. Wang, Y. Wang, Micro-heater on membrane with large uniform-temperature area, in: *Proceedings of IEEE Sensors Conference, 2006*, pp. 571–575.
- [31] A. Jain, K.E. Goodson, Measurement of the thermal conductivity and heat capacity of freestanding shape memory thin films using the  $3\omega$  method, *Journal of Heat Transfer* 130 (2008) 102402.
- [32] D. Pitts, L.E. Sissom, *Schuum's Outline of Heat Transfer*, second ed., McGraw-Hill, New York, 1998.
- [33] J. Courbat, M. Canonica, D. Teyssieux, D. Briand, N.F. de Rooij, Design and fabrication of micro-hotplates made on a polyimide foil: electrothermal simulation and characterization to achieve power consumption in the low mW range, *Journal of Micromechanics and Microengineering* 21 (2011) 015014.
- [34] X.J. Hu, A. Jain, K.E. Goodson, Investigation of the natural convection boundary condition in microfabricated structures, *International Journal of Thermal Sciences* 47 (2008) 820–824.
- [35] S. Astié, A.M. Gué, E. Scheid, J.P. Guillemet, Design of a low power SnO<sub>2</sub> gas sensor integrated on silicon oxynitride membrane, *Sensors and Actuators B: Chemical* 67 (2000) 84–88.
- [36] S.T. Inc., Heat transfer problem: heat transfer from a radial circular fin <http://www.syvum.com/cgi/online/serve.cgi/eng/heat/heat1003.html> (n.d.).
- [37] C. Falconi, A. D'Amico, C. Di Natale, M. Faccio, Low cost curvature correction of bandgap references for integrated sensors, *Sensors and Actuators A: Physical* 117 (2005) 127–136.
- [38] C. Falconi, M. Fratini, CMOS microsystems temperature control, *Sensors and Actuators B: Chemical* 129 (2008) 59–66.
- [39] N.M. Ravindra, S. Abedrabbo, W. Chen, F.M. Tong, A.K. Nanda, A.C. Speranza, Temperature-dependent emissivity of silicon-related materials and structures, *IEEE Transactions on Semiconductor Manufacturing* 11 (1998) 30–39.

## Biographies

**Usman Khan** was born in Pakistan and received B.Sc. degree in Electrical Engineering from the N.W.F.P University of Engineering and Technology (Peshawar, Pakistan) in 2006 and the M.Sc. degree in Electronic Engineering from GIK Institute of Engineering Sciences and Technology (Topi, District Swabi, Pakistan) in 2008. He is currently a Ph.D. student at the University of Tor Vergata. His research interests include sensors, actuators, thermal devices, and microsystems.

**Christian Falconi** was born in Rome, Italy, 1973. He received the M.Sc. (cum laude) and the Ph.D. degrees in Electronic Engineering from the University of Tor Vergata, Rome, Italy, in, respectively, 1998 and 2001; as a part of his Ph.D. program he visited the University of Linköping (1 month), and the Technical University of Delft (7 months). Since 2002 Christian Falconi is Assistant Professor at the Department of Electronic Engineering, University of Tor Vergata. Since 2003 he has been visiting the Georgia Institute of Technology (14 months). His research interests include semiconductor devices, analog electronics, electronic interfaces, sensors, microsystems, and nanosystems.